Core–Shell Nanostructures

DOI: 10.1002/anie.200703185

# Plasmon-Driven Synthesis of Triangular Core–Shell Nanoprisms from Gold Seeds**

*Can Xue, Jill E. Millstone, Shuyou Li, and Chad A. Mirkin**

*Dedicated to Professor David Reinhoudt on the occasion of his 65th birthday*

An interesting, unresolved issue in nanoscience involves the use of surface plasmon resonances (SPR) to influence nanocluster chemistry in a controllable manner. These electronic resonances have been studied for decades in the context of physical phenomena, such as plasmon coupling and waveguiding,[1,2] surface-enhanced Raman scattering (SERS),[3–6] and electromagnetic field-enhanced fluorescence.[7,8] More recently, they have been invoked in silver nanocluster synthesis,[9–12] for which surface plasmon excitation has been observed to control the growth of triangular prisms. In particular, it has been shown that Ag nanoprisms grow under irradiation until their dipole plasmon resonance is red-shifted relative to the excitation wavelength.[10] Although the photoinduced growth mechanism for silver nanoprisms is still under debate, we have proposed that this process is driven by plasmon excitation.[10] To investigate this hypothesis, we have developed a method in which we use pseudo-spherical gold nanoparticles as plasmonic cores and experimental labels to determine the role of plasmon excitation in the photochemical conversion of silver nanoparticles into nanoprisms. These experiments not only provide important insight into the significance of plasmon-mediated nanoprism growth but also have led to a new photochemical strategy for creating anisotropic shells on isotropic, plasmonic nanoparticle seeds, which results in a novel core–shell structure that has a spherical gold core and a triangular silver prism shell. Using this strategy, we can build composite nanostructures that have not been accessed by other methods. These discoveries unambiguously demonstrate that plasmon excitation plays a critical role in the growth of silver nanoprism structures and highlight the power and versatility of plasmon-mediated synthetic strategies.

In a typical experiment, colloidal gold and silver nanoparticles with diameters of 11 and 5 nm, respectively, were prepared according to literature protocols.[10,13] The dipole surface plasmon resonance bands of the gold and silver nanoparticles are located at 516 and 395 nm, respectively. Separate aqueous solutions of gold and silver nanoparticles were mixed to prepare a solution with a Au/Ag 1:10 particle ratio as determined by measuring optical density at the extinction maxima for such particles. The mixture was then irradiated with 550-nm light (bandpass filter, $550 \pm 20$ nm) for 5 h. The colloid was slowly centrifuged at 1200 rpm for 60 min to collect the nanoparticles (in the form of a pellet), which were then resuspended in an aqueous solution of trisodium citrate (0.3 mM). Transmission electron microscopy (TEM) shows that the resulting product consists of nanostructures (Figure 1a) that have triangular shells (average edge lengths of $70 \pm 6$ nm) and single-particle cores. The resulting nanostructures have a total thickness of 14 nm (Figure 1a, inset), and, significantly, there were no pure silver nanoprisms observed. High-resolution TEM shows that the triangular faces are [111] with a lattice spacing of 1.44 Å, indexed as {220} of fcc Ag (Figure 1c). The extinction bands at 632, 452, and 336 nm (as measured by UV/Vis spectroscopy) indicate that these core–shell nanoprisms have optical features similar to those of the pure silver prisms without gold cores.[10,14] The gold core and silver shell compositions were confirmed by

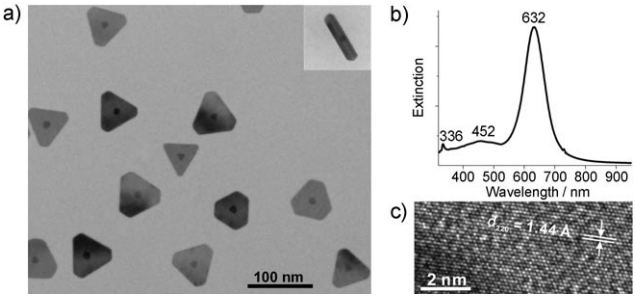


***Figure 1.*** a) A TEM image of the Au@Ag core–shell nanoprisms (average edge length of $70 \pm 6$ nm) synthesized by irradiation with 550-nm light. The inset shows the side view of a core–shell nanoprism. b) Extinction spectrum of the Au@Ag core–shell colloidal nanoprisms after centrifugation. c) A high-resolution TEM image of the [111] face of the Au@Ag core–shell nanoprisms. The hexagonal lattice shows a spacing of 1.44 Å, indexed as {220} of fcc Ag.

[*] C. Xue, J. E. Millstone, Prof. C. A. Mirkin
Department of Chemistry
International Institute for Nanotechnology
Northwestern University
2145 Sheridan Road, Evanston, IL 60208 (USA)
Fax: (+1) 847-467-5123
E-mail: chadnano@northwestern.edu
Dr. S. Li
Department of Material Science and Engineering
Northwestern University
2145 Sheridan Road, Evanston, IL 60208 (USA)

[**] This work was supported by the ONR, AFOSR, and MRSEC program of the National Science Foundation (DMR-0076097) at the Material Research Center of Northwestern University. C.A.M. is also grateful for an NIH Director's Pioneer Award.

Supporting information for this article is available on the WWW under http://www.angewandte.org or from the author.

energy-disperse X-ray spectroscopy (EDS, Figure 1S in the Supporting Information).

Time-resolved UV/Vis spectra reveal that as the gold core is coated with a silver shell during the first 30 min of irradiation, the surface plasmon resonance band of the composite nanostructure blue-shifts from 516 to 500 nm (Figure 2a). TEM analysis of the particles after this initial

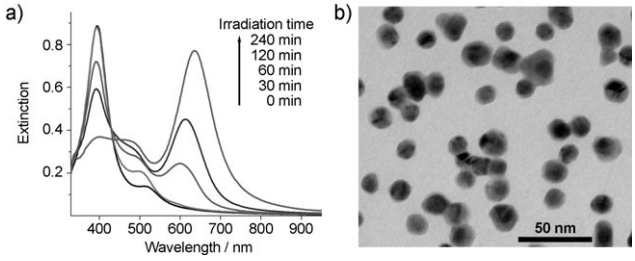


***Figure 2.*** a) Time-resolved extinction spectra of a solution of 11-nm gold and 5-nm silver nanoparticles irradiated with 550-nm light. b) A TEM image of the product after 30 min irradiation with 550-nm light.

irradiation period shows that the gold nanoparticles are covered by silver shells with irregular shapes (Figure 2b). During the next 30 min of irradiation, further silver deposition occurs, and the silver coating develops into a triangular shell. This process is easily characterized and followed by UV/Vis spectroscopy, which shows the appearance and progressive increase of a diagnostic triangular prism dipole resonance at approximately 600 nm.[9,14] The growth stops when the dipole plasmon resonance band of the core–shell triangular prism structure is red-shifted with respect to the excitation wavelength (Figure 2a).

High-resolution TEM images of the side planes of the core–shell prisms reveal that the number of twin planes varies (Figure 2S in the Supporting Information), which could be due to the nonuniformity of the gold nanoparticle seeds. Hexagonal shells and triangular shells with different degrees of truncation are also observed. These structures have likely not been fully transformed into triangular prisms[15] because of a depletion of the silver seed feedstock. Similar to the photo-induced growth of pure silver nanoprisms,[10] the silver shell growth on gold nanoparticles is also controlled by excitation wavelength. With longer excitation wavelengths (e.g. 600 nm), the triangular shells have larger average edge lengths ($80 \pm 7$ nm, Figure 3b). When 514-nm light (which almost coincides with the plasmon band of the gold nanoparticles) was used to excite the colloid, smaller triangular nanoprisms (average edge length of $48 \pm 5$ nm) and more hexagonal plates (Figure 3a) could be observed. Irradiation at wavelengths shorter than 514 nm (e.g. 488 nm) leads to an increase in irregular anisotropic particles with a low yield of core–shell nanoprisms.

Interestingly, the average thickness of these core–shell nanoprisms does not depend on the excitation wavelength. Rather, the thickness of the nanoprisms seems to be regulated by the diameter of the gold cores. For example, for 5-nm gold nanoparticles we observe triangular silver shell growth (Figure 4a) with a final prism thickness of $8 \pm 1$ nm. The

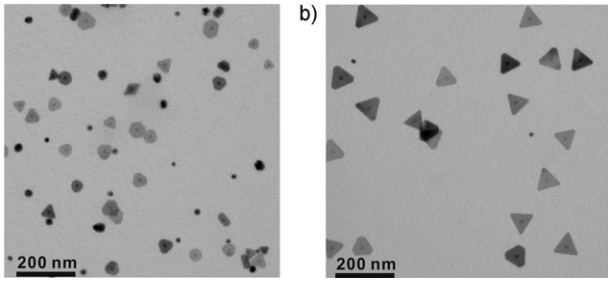


***Figure 3.*** TEM images of Au@Ag core–shell nanoprisms prepared through irradiation at a) 514 nm and b) 600 nm with average edge lengths of $48 \pm 5$ nm and $80 \pm 7$ nm, respectively.

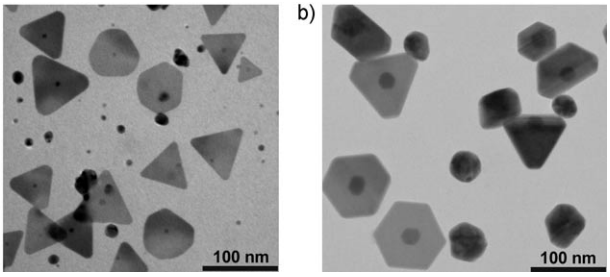


***Figure 4.*** Representative TEM images of the Au@Ag core–shell nanoprisms with core diameter of a) 5 nm and b) 25 nm.

contrast of the 5-nm gold cores in the silver prism shell is low, and the gold core could not be distinguished from the side planes. However, when larger gold particles (25-nm diameter) were used, the core–shell prism thickness was $30 \pm 3$ nm, although the overall yield of core–shell nanoprisms was lower than for prisms made with smaller gold cores, and a large population of irregular core–shell particles was observed (Figure 4b). This result may be due to the relatively high redox potential of large nanoparticles, which results in lower reactivity.[16]

The growth of these novel core–shell nanostructures is attributed to plasmon excitation and can be considered as a two-step pathway (first line, Figure 5). In the first step, the incident light preferentially excites the dipole plasmon resonance of the gold nanoparticles, which induces the deposition of silver layers (silver ions in the solution come from the dissolution of small silver nanoparticles), because the SPR band of gold nanoparticles (516 nm) is closer to the excitation wavelength (550 nm) than that of the silver nanospheres (395 nm). Consistent with this hypothesis, the SPR band of the silver-coated gold nanoparticles blue-shifts from 516 to 500 nm with increased band intensity, thus indicating that these nanoparticles exhibit hybrid optical features of gold and silver. The use of the Ag particles as a feedstock for $Ag^+$ is significant. The low redox potential of 5-nm Ag nanoparticles compared with the Au@Ag core–shell nanostructures[16,17] allows the preferential oxidation and dissolution of the silver nanoparticles. This process keeps the concentration of $Ag^+$ low but consistent throughout the photochemically induced $Ag^+$ reduction and deposition onto the gold surfaces. Such core–shell structures can be synthesized using $AgNO_3$ as

  

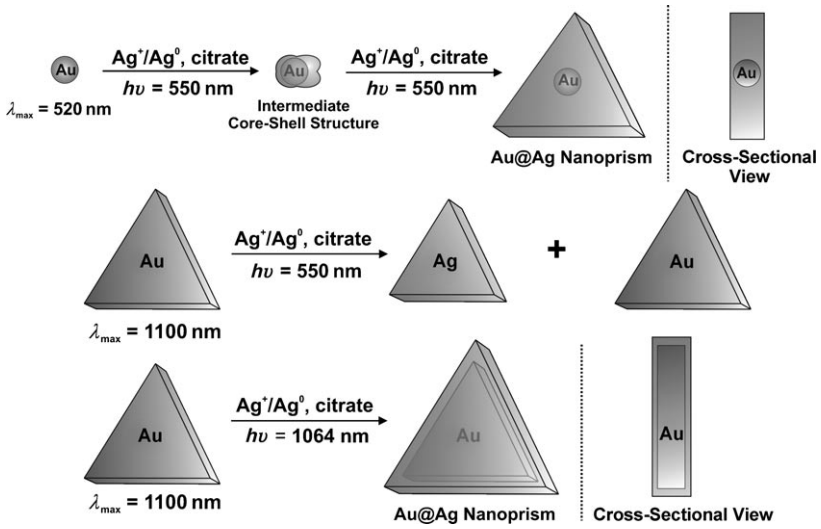


***Figure 5.*** Schematic illustration of the growth pathways for the Au@Ag core–shell nanostructures.

the silver source, but the reaction and the quality of the resulting prisms are more difficult to control.

In the early stage of core–shell particle growth, the silver shell begins to exhibit an anisotropic morphology (Figures 2b and 5), but it does not have the same morphology for each particle in solution. This early dispersity in nanoparticle architecture may be due in part to momentary differences in electric field polarization across the nanoparticle surface during excitation,[14] which could play a role in the local redox chemistry. As the extinction bands of these Au@Ag particles approach the excitation wavelength, further excitation leads to the reconstruction of surface silver atoms into prismatic shells, possibly by the mechanism proposed by Brus.[18] However, we do not observe changes in the morphology of gold nanoparticles over the course of these experiments. The growth of silver triangular shells does not show specific dependence on the shape and symmetry of gold cores. From these data, we hypothesize that the plasmon excitation leads to deposition of silver layers on the gold nanoparticle surface and creates Ag [111] twin planes. With continuing plasmon excitation, further silver shell growth accelerates in the direction of the parallel twin planes, while growth on the direction perpendicular to the [111] planes is much slower. Such a growth pattern leads to three-fold symmetry, which results in small trigonal or hexagonal silver shells. These prismatic shells will continue to grow until the final structures no longer absorb the wavelength of irradiation (Figure 5).[9]

We also have explored plasmon-excitation-mediated deposition of Ag on Au particle seeds[19] that exhibit surface plasmon resonances in the near-IR region of the spectrum. These seeds are prisms with plasmon resonances that do not overlap with the Ag nanoprism optical features in the visible region of the spectrum. This experiment allows us to probe the role of seed plasmon excitation in silver deposition and eventual triangular shell formation. With NIR excitation using a 1064-nm band-pass filter, core–shell nanoprisms with triangular gold cores and triangular silver shells form (Figures 5 and 6). Significantly, in a control experiment, when the seed solution was irradiated with 550-nm light, only silver nanoprisms without gold cores form. These results show that it is, indeed, the activation of the plasmonic core by SPR excitation that leads to preferential silver deposition on the gold core and subsequent triangular silver shell growth.

The photochemical mechanism of plasmon-induced particle growth is quite complex and can be viewed in one of two ways. Some have proposed that it involves the excitation of the particle followed by charge transfer between the adsorbates ($Ag^+$ and citrate) and the hot electrons (holes and stronger reducing equivalents).[20–22] In this case, the gold is behaving as a photocatalyst, which is common for semiconductors but uncommon for metals.[23] However, the redox chemistry of $Ag^+$ and citrate is thermodynamically downhill based upon their redox potentials ($E_{Ag+/Ag} = 0.7996$ V vs. normal hydrogen electrode, and $E_{ADE,\,CO_2/citrate} < -0.01$ V at pH > 8[23]), and photoexcitation of a photocatalyst is not necessary to effect the redox reaction. In fact, aqueous $AgNO_3$ and citrate will react at 100 °C in the dark to form silver particles, $CO_2$, and 1,3-acetonedicarboxylate (ADE, the oxidation product of citrate). Therefore, we must also consider the possibility that the photoexcitation of the particle simply results in a catalyst that facilitates the reaction between $Ag^+$ and citrate, perhaps through photoinduced ligand rearrangement or ligand dissociation at the surface of the particle. Although it is challenging to completely differentiate these subtly but fundamentally different processes, we believe that the latter is unlikely. This conclusion is based upon the observation that citrate and $Ag^+$ are indefinitely stable (at least one month) in the presence of the gold particles. When we consider that the citrate is weakly bound to the surface of the Au nanoparticle seeds, it is difficult to believe that the particle is simply acting as a

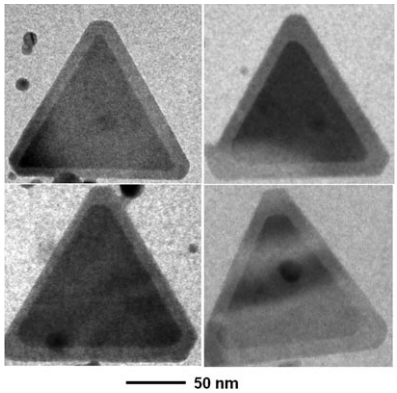


***Figure 6.*** Representative TEM images of Au@Ag core–shell nanoprisms with a gold prism core. The scale bar is the same for all images.

  

precatalyst activated by ligand dissociation, since we would expect to see some background catalytic activity in the dark.

This work is significant for the following reasons. First, these experiments clearly demonstrate the role of seed plasmon excitation in the photochemical synthesis of Au@Ag core–shell prism structures and, by analogy, of pure silver structures. Our method illustrates a new way to probe and track photomediated processes using plasmonic cores as reaction labels. Finally, the method leads to novel core–shell nanostructures that would be difficult to synthesize by other methods. These structures have architectures that are easily tuned by controlling excitation wavelength and core diameter. Taken together, these results provide significant insight into the mechanism of photochemical colloid synthesis and demonstrate the flexibility and utility of photomediated methods for the synthesis of novel nanostructures.

Received: July 16, 2007
Revised: August 16, 2007
Published online: October 2, 2007

**Keywords:** core–shell particles · nanostructures · photochemistry · silver · surface plasmon resonance

[1] A. W. Sanders, D. A. Routenberg, B. J. Wiley, Y. N. Xia, E. R. Dufresne, M. A. Reed, *Nano Lett.* **2006**, *6*, 1822.
[2] P. K. Jain, S. Eustis, M. A. El-Sayed, *J. Phys. Chem. B* **2006**, *110*, 18243.
[3] S. E. Hunyadi, C. J. Murphy, *J. Mater. Chem.* **2006**, *16*, 3929.
[4] H. Wang, C. S. Levin, N. J. Halas, *J. Am. Chem. Soc.* **2005**, *127*, 14992.
[5] L. D. Qin, S. L. Zou, C. Xue, A. Atkinson, G. C. Schatz, C. A. Mirkin, *Proc. Natl. Acad. Sci. USA* **2006**, *103*, 13300.
[6] J. M. McLellan, Z. Y. Li, A. R. Siekkinen, Y. N. Xia, *Nano Lett.* **2007**, *7*, 1013.
[7] K. Aslan, M. Wu, J. R. Lakowicz, C. D. Geddes, *J. Am. Chem. Soc.* **2007**, *129*, 1524.
[8] F. Tam, G. P. Goodrich, B. R. Johnson, N. J. Halas, *Nano Lett.* **2007**, *7*, 496.
[9] R. C. Jin, Y. W. Cao, C. A. Mirkin, K. L. Kelly, G. C. Schatz, J. G. Zheng, *Science* **2001**, *294*, 1901.
[10] R. C. Jin, Y. C. Cao, E. C. Hao, G. S. Metraux, G. C. Schatz, C. A. Mirkin, *Nature* **2003**, *425*, 487.
[11] V. Bastys, I. Pastoriza-Santos, B. Rodriguez-Gonzalez, R. Vaisnoras, L. M. Liz-Marzan, *Adv. Funct. Mater.* **2006**, *16*, 766.
[12] C. Xue, C. A. Mirkin, *Angew. Chem.* **2007**, *119*, 2082; *Angew. Chem. Int. Ed.* **2007**, *46*, 2036.
[13] K. C. Grabar, R. G. Freeman, M. B. Hommer, M. J. Natan, *Anal. Chem.* **1995**, *67*, 735.
[14] K. L. Kelly, E. Coronado, L. L. Zhao, G. C. Schatz, *J. Phys. Chem. B* **2003**, *107*, 668.
[15] C. Lofton, W. Sigmund, *Adv. Funct. Mater.* **2005**, *15*, 1197.
[16] N. R. Jana, L. Gearheart, C. J. Murphy, *Chem. Mater.* **2001**, *13*, 2313.
[17] N. K. Chaki, J. Sharma, A. B. Mandle, I. S. Mulla, R. Pasricha, K. Vijayamohanan, *Phys. Chem. Chem. Phys.* **2004**, *6*, 1304.
[18] M. Maillard, P. R. Huang, L. Brus, *Nano Lett.* **2003**, *3*, 1611.
[19] J. E. Millstone, G. S. Metraux, C. A. Mirkin, *Adv. Funct. Mater.* **2006**, *16*, 1209.
[20] P. L. Redmond, E. C. Walter, L. E. Brus, *J. Phys. Chem. B* **2006**, *110*, 25158.
[21] C. D. Lindstrom, X. Y. Zhu, *Chem. Rev.* **2006**, *106*, 4281.
[22] K. Watanabe, D. Menzel, N. Nilius, H. J. Freund, *Chem. Rev.* **2006**, *106*, 4301.
[23] G. Trettenhahn, A. Koberl, *Electrochim. Acta* **2007**, *52*, 2716.

  